

A Study on Peak-to-Average Power Ratio in DWT-OFDM Systems

Filbert H. Juwono^{*}, Randy S. Putra, and Dadang Gunawan

Department of Electrical Engineering, University of Indonesia
Kampus Baru UI Depok, 16424

^{*}Corresponding author, e-mail: filbert@ieee.org

Abstract

Orthogonal frequency division multiplexing (OFDM) systems suffer from large peak-to-average power ratio (PAPR). In this paper we study the discrete wavelet transform (DWT)-based OFDM systems. In particular, we discuss the effect of the decomposition level of each wavelet family in the DWT-based OFDM regarding the PAPR. The simulation results show that, in general, there is a decomposition level that minimize the PAPR in every wavelet family. In addition, we also analyze the effect of clipping nonlinearities, i.e. conventional clipping and deep clipping, as PAPR reduction method in DWT-OFDM systems. The results show that the clipping nonlinearities give a noticeable PAPR reduction. However, as DWT-OFDM itself has lower PAPR compared to the conventional discrete Fourier transform (DFT)-based OFDM, the clipping nonlinearity subsystem may not be essential as it degrades the system performance.

Keywords: OFDM, PAPR, DWT-OFDM

Copyright © 2014 Institute of Advanced Engineering and Science. All rights reserved.

1. Introduction

Orthogonal frequency division multiplexing (OFDM) is a popular modulation technique for broadband services in wireless communications, such as DVB-T [1] and wireline communications, such as optical communications [2] and power line communications [3]. OFDM divides the total bandwidth into some parallel narrowband subcarriers so that the symbol duration, T_s , is smaller than the multipath delay. As a result, it overcomes intersymbol interference (ISI) problem in multipath fading environment.

However, OFDM also has two main drawbacks, i.e. the sensitivity to frequency offset and large peak-to-average power ratio (PAPR). Frequency offset deals with loss of the orthogonality between subcarriers [4]. Meanwhile, large PAPR causes inefficiency in power amplifier. In OFDM-based communication systems, PAPR reduction is needed to perform power savings [5].

Some PAPR reduction methods have been proposed. Generally, the reduction methods can be divided into three categories: distortion method, such as clipping and filtering; distortionless or probabilistic method, such as selective mapping; and coding method such as Golay complementary sequences [6]. An overview of some PAPR reduction methods can be found in [7].

All the PAPR reduction methods described in [7] deal with discrete Fourier transform (DFT)-based OFDM. Another variant of OFDM, called discrete wavelet transform (DWT)-based OFDM, was studied in [8–10]. In particular, DWT-OFDM was basically intended to deal with the narrowband interference as well as intercarrier intersymbol (ICI) [8]. In contrast to DFT-OFDM, no cyclic prefix (CP) is needed in DWT-OFDM so that improving the spectral efficiency [9, 10]. Moreover, the use of DWT in place of DFT can also reduce PAPR [8].

In [8], DWT-OFDM systems with three wavelet functions were compared in terms of PAPR distribution. The wavelet functions used were daubechies 1 (Haar), symlets, and coiflets. The simulation results showed that the Haar wavelet yielded the minimum PAPR. However, the effect of decomposition level for each wavelet family regarding the PAPR distribution has not been discussed in [8]. In this paper, we will simulate the distribution of the PAPR for every decomposition level to obtain the best decomposition level for each wavelet family, i.e. the decomposition

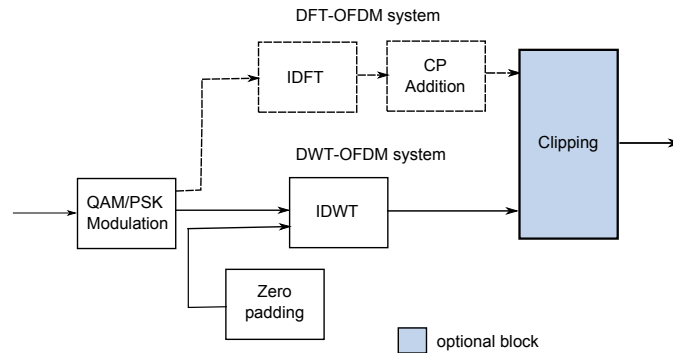


Figure 1. DFT- and DWT-OFDM System

level that yields the lowest PAPR. In addition, clipping nonlinearity subsystem may be added in the DWT-OFDM systems to obtain more PAPR reduction. We will show the simulation results for PAPR distribution of a DWT-OFDM system using two clipping nonlinearity functions, i.e. conventional clipping and deep clipping and compare them with DWT-OFDM and DFT-OFDM systems.

The rest of this paper is organized as follows. Section II discusses the DFT-based and DWT-based OFDM system models. Section III compares and analyzes the simulation results. The conclusions are given in Section IV.

2. System Model

2.1. DFT- and DWT-OFDM

The k -th unmodulated parallel subcarrier signal in OFDM systems is given by [12]

$$\tilde{g}_k(t) = \begin{cases} e^{j2\pi k\Delta ft}, & \text{if } \forall t \in [0, T_s], \\ 0, & \text{if } \forall t \notin [0, T_s]. \end{cases} \quad (1)$$

To overcome interblock intersymbol (IBI), a guard interval in form of CP is appended in the front of each OFDM block so that the subcarrier signal becomes

$$g_k(t) = \begin{cases} e^{j2\pi k\Delta ft}, & \text{if } \forall t \in [-T_g, T_s], \\ 0, & \text{if } \forall t \notin [-T_g, T_s]. \end{cases} \quad (2)$$

where T_g is the CP length.

Therefore, the analog OFDM signal can be expressed as

$$x(t) = \frac{1}{\sqrt{N}} \sum_{k=0}^{N-1} X_k e^{j\frac{2\pi kt}{T_s}} \quad (3)$$

where N is the number of subcarriers, X_k is the QAM/PSK modulated signal, and $j = \sqrt{-1}$. From (3) it is obvious that we can implement the inverse discrete Fourier transform (IDFT), so named DFT-OFDM, to the modulated input signal X_k to obtain the OFDM signal. The discrete DFT-OFDM can be obtained by sampling the analog OFDM signal at time $x[n] = x(nT_s/N)$.

Another way to form OFDM signal is to replace the IDFT by inverse discrete wavelet transform (IDWT) [8–11]. DFT- and DWT-OFDM systems are shown in Fig. 1. CP is not required in DWT-OFDM system as mentioned before. A clipping subsystem can be optionally added. We will discuss the discrete wavelet transform in the next subsection.

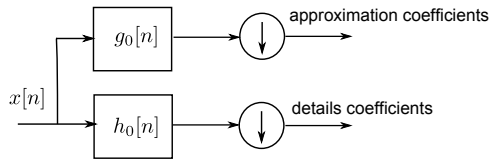


Figure 2. DWT decomposition

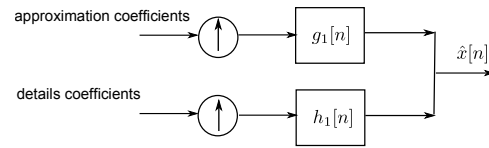


Figure 3. DWT reconstruction

2.2. Discrete Wavelet Transform

As the discrete transforms are basically the sampled version of the continuous transforms, we will first present the continuous wavelet transform (CWT). CWT can be expressed as [13]

$$W(a, b) = \int_{-\infty}^{\infty} f(t) \frac{1}{\sqrt{|a|}} \psi^* \left(\frac{t-b}{a} \right) dt \quad (4)$$

where $\psi(t)$ is mother wavelet, $f(t)$ is the input signal, and * denotes complex conjugate operator. The inverse of the wavelet transform can be expressed as

$$f(t) = \frac{1}{C} \int_{-\infty}^{\infty} \int_{-\infty}^{\infty} \frac{1}{|a|^2} W(a, b) \frac{1}{\sqrt{|a|}} \psi \left(\frac{t-b}{a} \right) da db \quad (5)$$

where

$$C = \int_{-\infty}^{\infty} \frac{|\Psi|^2}{|\omega|} d\omega$$

and

$$\Psi(\omega) = \int_{-\infty}^{\infty} \psi(t) e^{-j\omega t} dt$$

The mother wavelet must satisfy the three properties:

1. The total area under the $\psi(t)$ is zero. This implies that the function must oscillate above and below the x -axis.

$$\int_{-\infty}^{\infty} \psi(t) dt = 0 \quad (6a)$$

2. The total area of $|\psi(t)|^2$ is finite that implies the energy of the wavelet is finite.

$$\int_{-\infty}^{\infty} |\psi(t)|^2 dt < \infty \quad (6b)$$

3. The admissibility condition which means C is required to be positive and finite.

As shown in (4), the CWT involves time shifting and scaling factor. In DWT, those operations are implemented by using the lowpass and highpass filters which are denoted by $g[n]$ and $h[n]$, respectively. The decomposition and reconstruction (inverse) filters of DWT are shown in Fig. 2 and Fig. 3, respectively.

In Fig. 2, input signal samples are convolved with the lowpass and highpass decomposition filter coefficients and then they are downsampled by a factor of two. As a result, we have approximation and details coefficients. To do the reconstruction process, as shown in Fig. 3, an upsampling process by factor of two is applied and then followed by a convolution process with highpass and lowpass reconstruction filters coefficients.

Table 1. Wavelet families used in this paper

Wavelet Families	Wavelet Function with Orders
Daubechies (Db)	Db1, Db3, Db5, Db7, Db9, Db11
Symlets (sym)	sym1, sym3, sym5, sym7, sym9
Coiflets (coif)	coif1, coif2, coif3, coif4, coif5
BiorSplines (bior) and ReverseBior (rbio)	bior5.5, bior6.8, rbio3.7, rbio3.9, rbio4.4, rbio5.5, rbio6.8

2.3. Wavelet Families

As discussed in the previous subsection, mother wavelet can be any function as long as it satisfies the three properties. In general, there are two categories of wavelet families: orthogonal and biorthogonal [13–15]. The orthogonality of the wavelet family deals with the filter coefficients. The orthogonal wavelet family includes Daubechies (Db), Symlet (sym), and Coiflet (coif) while the biorthogonal wavelets are BiorSplines (bior) and ReverseBior (rbio). Orthogonal wavelet is characterized by a parameter \mathcal{N} which is the filter order while biorthogonal wavelet may have different order for the decomposition and reconstruction filters, i.e. \mathcal{N}_d and \mathcal{N}_r , respectively [16]. The wavelet families used in this paper are summarized in Table.1.

2.4. Clipping Nonlinearity

In this paper we use two clipping nonlinearity functions, which are conventional clipping and deep clipping [17]. The conventional clipping formula is given by

$$y[n] = \begin{cases} x[n], & \text{if } |x[n]| \leq T, \\ Te^{j\varphi[n]}, & \text{if } |x[n]| > T. \end{cases} \quad (7)$$

where T is clipping threshold and $\varphi[n] = \arg x[n]$. The formula for deep clipping is

$$y[n] = \begin{cases} x[n], & \text{if } |x[n]| \leq T, \\ T - p(|x[n]| - T)e^{j\varphi[n]}, & \text{if } T < |x[n]| \leq \beta T, \\ 0, & \text{if } |x[n]| > \beta T. \end{cases} \quad (8)$$

where p is depth factor and $\beta = (p + 1)/p$. The clipping threshold is characterized by a parameter called clipping ratio which is defined as

$$CR = \frac{T}{\sigma} \quad (9)$$

where σ is the rms of the OFDM signal.

3. Results and Analysis

In this simulation, we use 16-QAM modulation, 64 subcarriers, and four times oversampling. To analyze PAPR distribution, a statistical parameter called complementary cumulative distribution function (CCDF) is usually used. CCDF gives a probability that PAPR exceeds certain value. The CCDF results for DWT-OFDM systems using orthogonal wavelet families, i.e. Db, sym, coif, compared with DFT-OFDM are shown in Fig. 4 - Fig. 6, respectively.

We can observe from Fig. 4 that DWT-OFDM using Db1 has the lowest PAPR. The difference is about 7.5 dB at probability of 10^{-3} compared with the conventional DFT-OFDM. Note that the levels of PAPR for odd-order Daubechies wavelet family, from Db3 to Db11, do not linearly depend on the filter order. In Fig. 5, at probability of 10^{-3} the lowest PAPR distribution in DWT-OFDM is achieved by using sym1, which is about 7.5 dB lower than DFT-OFDM, and it is the same as DWT-OFDM using Db1 system. Meanwhile, the PAPR distributions of DWT-OFDM using sym3, sym5, sym7, and sym9 are nearly the same, which is about 4.5 dB lower than DFT-OFDM

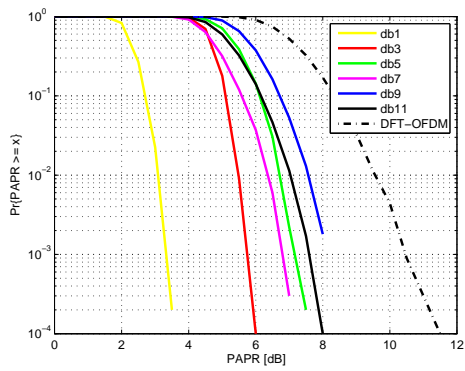


Figure 4. CCDFs of PAPR for Daubechies DWT- and DFT-OFDM

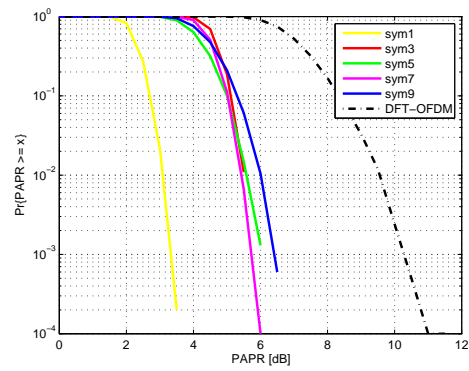


Figure 5. CCDFs of PAPR for symlet DWT- and DFT-OFDM

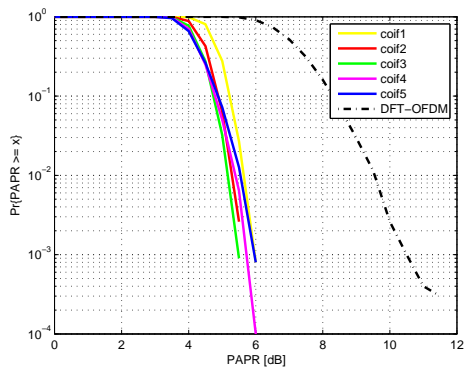


Figure 6. CCDFs of PAPR for coiflet DWT- and DFT-OFDM

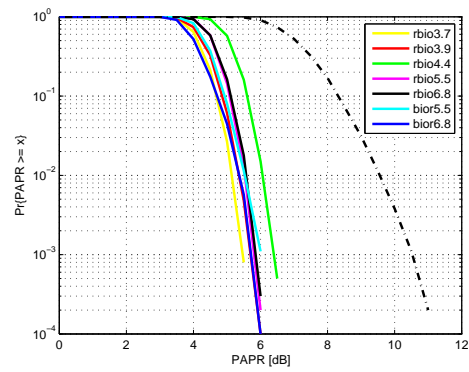


Figure 7. CCDFs of PAPR for biorthogonal DWT- and DFT-OFDM

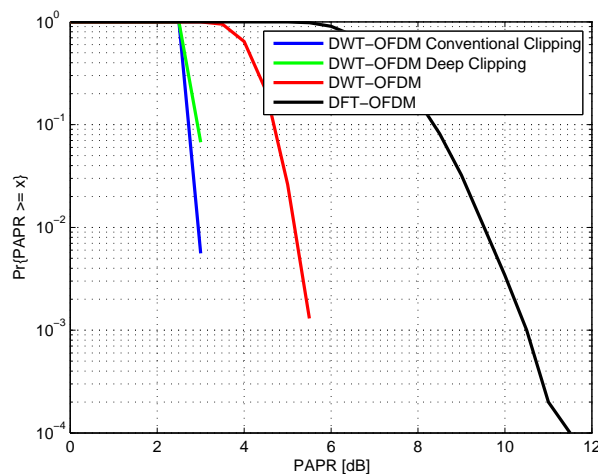


Figure 8. CCDFs of PAPR for DWT- and DFT-OFDM with clipping nonlinearity

at probability of 10^{-3} . As shown in Fig. 6, the PAPR distributions of DWT-OFDM using *coif1-coif5* have only little difference. However, we can observe that DWT-OFDM using *coif3* has the lowest PAPR compared with DFT-OFDM which is about 5 dB difference at probability of 10^{-3} .

Fig. 7 shows the CCDF for biorthogonal wavelet families compared with DFT-OFDM. It is obvious that all the results using biorthogonal wavelet functions yield almost the same PAPR distribution. At probability of 10^{-3} , *rbio3.7* yields about 5 dB reduction compared with DFT-OFDM.

In Fig. 8, we analyze the effect of clipping nonlinearity functions in DWT-OFDM and also compared it with DFT-OFDM. We use conventional clipping and deep clipping with $p = 0.6$. The clipping ratio, CR , is set to be 1.4 for both clipping functions. We use *rbio3.7* wavelet function for this simulation. We notice that the clipping nonlinearity gives additional PAPR reduction, about 2 dB, compared with the DWT-OFDM system. Additionally, conventional clipping and deep clipping have nearly similar results. As the DWT-OFDM systems have smaller PAPR than DFT-OFDM systems, it is not necessary to perform an additional PAPR reduction technique by using clipping nonlinearity because it degrades the system performance. Therefore, DWT-OFDM systems offer an advantage compared with the DFT-OFDM systems regarding the PAPR distribution.

4. Conclusions

We have simulated the DWT-OFDM using orthogonal and biorthogonal wavelet families. The simulation results show that DWT-OFDM reduces the PAPR compared with conventional DFT-OFDM. For each wavelet family, the effect of decomposition level (or filter order) is also compared. For orthogonal wavelet family, the *Db1*, *sym1*, and *coif3* yield the largest PAPR reduction while for biorthogonal wavelet, the *rbio3.7* yields the largest PAPR reduction. Finally, as DWT-OFDM reduces the PAPR significantly, the clipping nonlinearity subsystem is not desirable since the system performance is not expected to degrade at the receiver.

References

- [1] E. Costa and S. Pupolin, "M-QAM-OFDM System Performance in the Presence of a Nonlinear Amplifier and Phase Noise," *IEEE Trans. Comm.*, vol. 50, no. 3, pp. 462-472, 2002.
- [2] J. Armstrong, "OFDM for Optical Communications," *Journal of Lightwave Technology*, vol. 27, no. 3, pp. 189-204, 2009.
- [3] S. Galli, A. Scaglione, and Z. Wang, "For the Grid and Through the Grid: The Role of Power Line Communications in the Smart Grid," *Proc. IEEE*, Vol. 99, no. 6, pp. 998-1027, 2011.

- [4] P. Dharmawansa, N. Rajatheva, and H. Minn, "An Exact Error Probability Analysis of OFDM Systems with Frequency Offset," *IEEE Trans. Comm*, vol. 57, no. 1, pp. 26-31, 2009.
- [5] R. J. Baxley and G. T. Zhou, "Power Savings Analysis of Peak-to-Average Power Ratio Reduction in OFDM," *IEEE Trans. Consum. Electron.*, vol. 50, no. 3, pp. 792-798, 2004.
- [6] F. H. Juwono and D. Gunawan, "PAPR Reduction Using Huffman Coding Combined with Clipping and Filtering for OFDM Transmitter," in *Conf. Innovative Technologies in Intelligent Systems and Industrial Applications*, 2009.
- [7] S. H. Han and J. H. Lee, "An Overview of Peak-to-Average Power Ratio Reduction Techniques for Multicarrier Transmission," in *IEEE Wireless Comm.*, vol. 12, no. 2, pp. 56-65, 2005.
- [8] S. Khalid and S. I. Shah, "PAPR Reduction by Using Discrete Wavelet Transform," in *2nd Int. Conf. Emerging Technologies*, 2006.
- [9] K. Abdullah and Z. M. Hussain, "Studies on DWT-OFDM and FFT-OFDM Systems," in *Int. Conf. Communication, Computer, and Power*, 2009.
- [10] K. Abdullah, A. Z. Sadik, and Z. M. Hussain, "On the DWT- and WPT-OFDM versus FFT-OFDM," in *GCC Conf. and Exhibitions*, 2009.
- [11] K. Abdullah and Z. M. Hussain, *Simulation of Models and BER Performances of DWT-OFDM versus FFT-OFDM in Discrete Wavelet Transform - Algorithm and Applications*. InTech, Croatia, 2011.
- [12] H. Rohling. *OFDM: Concept for Future Communication Systems*. Springer, Berlin, 2011.
- [13] D. Salomon. *Data Compression, 4th. Ed*. Springer, London, 2007.
- [14] M. Misiti, Y. Misiti, G. Oppenheim, and J-M. Poggi. *Wavelets and Their Applications*. ISTE, London, 2007.
- [15] A. Phinyomark, C. Limsakul, and P. Phukpattaranont, "An Optimal Wavelet Function Based on Wavelet Denoising for Multifunction Myoelectric Control," in *6th Int. Conf. Electrical Engineering/Electronics, Computer, Telecommunications and Information Technology*, 2009.
- [16] G. K. Kharate, V. H. Patil, and N. L. Bhale, "Selection of Mother Wavelet For Image Compression on Basis of Image," in *Journal of Multimedia*, vol. 2, no. 6, pp. 44-52, 2007.
- [17] D. Guel and J. Palicot, "Analysis and Comparison of Clipping Techniques for OFDM Peak-to-Average Power Ratio Reduction," in *Int. Conf. Digital Signal Processing*, 2009.